Impact of Polymer Microstructure on the Self-Assembly of Amphiphilic Polymers in Aqueous Solutions

Roger C. W. Liu, Agnès Pallier, Marc Brestaz, Nadège Pantoustier, and Christophe Tribet*

Laboratoire de Physico-Chimie des Polymères et des Milieux Dispersés, CNRS UMR 7615, ESPCI, 10 rue Vauquelin, F-75005 Paris, France

Received February 14, 2007; Revised Manuscript Received March 30, 2007

ABSTRACT: A new series of amphiphilic polymers (amphipols) with varied molecular characteristics was prepared, and their properties in aqueous media were examined by static and dynamic light scattering techniques. These polymers are short poly(sodium methacrylate) chains of various molecular weights and tacticities, modified with different degrees of *n*-octylamine as copolymers of two distinct hydrophobe distribution sequences (random vs multiblocky). To synthesize the parent poly(methacrylic acid) (PMAA) prior to hydrophobic modification, *tert*-butyl methacrylate was polymerized under the controlled conditions of atom transfer radical polymerization (ATRP) to yield after deprotection the syndiotactic-rich PMAA of targeted molar masses (12−28 kg mol^{-1}) and low polydispersity indexes (1.08−1.19). Under similar conditions of ATRP and deprotection, a well-defined isotactic-rich PMAA was obtained from triphenylmethyl methacrylate. The amphipol carrying octyl side chains randomly distributed along the polymer main chain was produced by coupling the parent PMAA with *n*-octylamine in an organic medium (*N*-methylpyrrolidone). In contrast, the coupling reaction of PMAA in aqueous media, with the *n*-octylamine solubilized by sodium dodecyl sulfate, gave the amphipols bearing octyl groups distributed in a multiblocky fashion. The highly controlled hydrophobe distribution sequence and polymer tacticity were confirmed by ^{1}H and ^{13}C NMR spectroscopic techniques. All polymers in aqueous solutions form nanoparticles with the structure strongly determined by the polymer microstructure and composition. In the case of random graft amphipol, the polymer self-assembles and preferentially forms small aggregates of 1−2 polymer chains on average with a hydrodynamic radius of ∼3 nm. In cases of the multiblocky graft amphipols, well-defined nanoscaled self-assemblies are formed but from multiple polymer chains (aggregation number = ∼17), with a drastic increase in the hydrodynamic radius (∼13 nm). Comparing to the effects due solely to the hydrophobe distribution sequence, the increments in structural parameters of the amphipol self-assemblies are only slightly enhanced when concurrently improving the polymer isotacticity or increasing the polymer molar mass. All results point to the critical impact of hydrophobe distribution sequence on the self-assembly of methacrylate-based amphipols in aqueous solutions.

Introduction

Self-association in aqueous solutions is a characteristic common to many water-soluble amphiphilic polymers.[1] These polymers undergo intrapolymeric or interpolymeric hydrophobic associations or at the same time both types of associations to form micelle-like assemblies,[2] vesicles called polymersomes,[3] or transient networks.[4] Many applications involving these associations are found in different fields,[5] such as enhanced oil recovery fluids, personal care formulations, and water-borne paints. Other developments involve the hydrophobic associations of amphiphilic polymers but with water-insoluble biomolecules or biomacromolecules for drug delivery systems and applications in protein stabilization.[6] To provide such functionalities, amphiphilic polymers are generally composed of hydrophilic repeating units that give the polymer water solubility and of hydrophobic repeating units that induce the polymer self-associations or hydrophobic interactions in water.[7] In some special cases, the amphiphilic polymers coined as polysoaps possess the amphiphilic surfactant-like repeating units, which mostly induce intrapolymeric hydrophobic associations.[8] We focus here on the impact of distribution sequence of these hydrophobic repeating units among the hydrophilic ones on the self-association of amphiphilic copolymers and study as well the influence of additional polymer structural parameters like polymer molecular weight, polydispersity, tacticity, and the incorporation level of the hydrophobic repeating units.

In general, the self-association and thus the physical properties of amphiphilic polymers are governed by the balance between hydrophobicity and hydrophilicity of the polymer chain itself,[9] which is controlled by the polymer chemical composition and microstructure. To shift the polymer hydrophobic−hydrophilic balance, the incorporation level of hydrophobic repeating units is widely used as a variable parameter, which however unavoidably adjusts the polymer hydrophobicity and inversely the hydrophilicity at the same time. Other commonly used methods include the integration of hydrophobes of different lengths and bulkinesses,[10] the use of neutral hydrophilic repeating units together with the ionizable ones,[11] and the introduction of external stimuli by varying the solution pH, temperature, and ionic strength.[12] Even so, it is reported that the hydrophobic−hydrophilic balance, even of linear polymer chains, cannot simply be captured by the average polymer chemical composition.[13] Specifically, Candau et al. have shown that the presence of short blocks of hydrophobes instead of randomly distributed hydrophobes increases notably the persistence time of physical cross-links in the poly(acrylamide-*co*-alkylacrylamide) gels,[14] revealing the significance of polymer microstructure (hydrophobe distribution sequence).[15]

How the distribution sequence of hydrophilic and hydrophobic monomers affects the morphology is also exemplified by the studies of diblock vs triblock copolymers. Amphiphilic diblock

* Corresponding author. E-mail: christophe.tribet@espci.fr.

10.1021/ma070397s CCC: $37.00 © 2007 American Chemical Society
Published on Web 05/16/2007

Scheme 1. Synthetic Routes to the Amphipols with Varied Structural Parameters

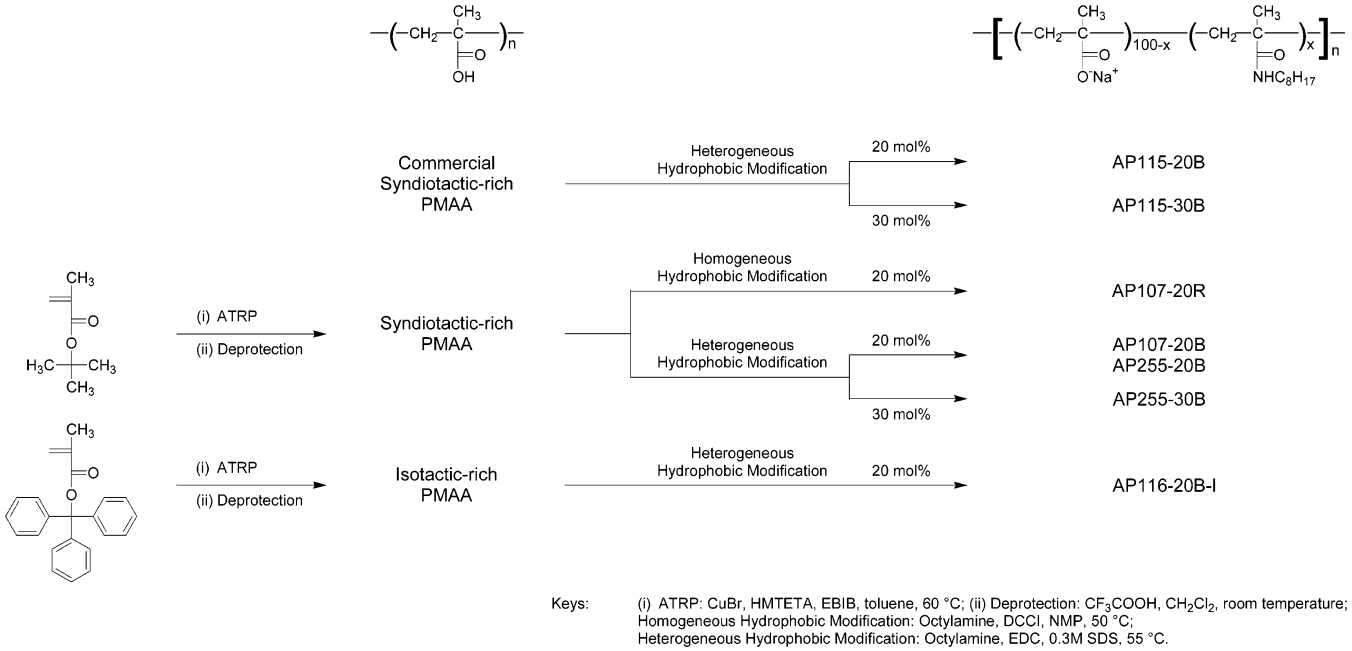

copolymers bearing a block of hydrophilic monomers and a block of hydrophobic monomers are known to form well-defined spherical micelles with a hydrophobic core and a hydrophilic shell.[16] However, amphiphilic triblock copolymers that carry a hydrophilic block in between two hydrophobic blocks form well-defined flowerlike micelles,[17] with the hydrophobic core protected by the hydrophilic loops. In either case, the polydispersity of micelles is low and the size is barely varied with the polymer concentration, although the telechelic structure in the latter case brings possibly some connectivity to the system that bridges the micelles,[18] which in turn form self-aggregates with multiple size distributions.[19] In contrast, when the hydrophobic monomers are distributed statistically along the main chain of hydrophilic monomers, the corresponding amphiphilic random copolymers rather form ill-organized micelle-like clusters, with a broad size distribution and the presence of multiple nanosized hydrophobic domains.[20] Unusual examples have been reported on random copolymers, which are polymers based on sodium 2-acrylamido-2-methylpropanesulfonate incorporating with a high level of alkyl-substituted methacrylamides, that form well-defined micelles, preferably undergo intrapolymeric self-associations, and form concentration-independent unimolecular micelles (unimers).[21] We recently reported the formation of well-defined self-aggregates from a polydispersed readily water-soluble random terpolymer of sodium acrylate, isopropylacrylamide, and octylacrylamide, which belongs to a group of amphiphilic polymers called amphipols that are especially designed for membrane protein stabilization.[22]

Aiming at identifying the parameters that affect the formation and size of micelle-like clusters of chains, we report in this paper the synthesis, characterization, and a comparative study on the self-association in aqueous solutions of a new series of sodium methacrylate-based amphipols bearing diverse structural characteristics, which are the hydrophobe distribution sequence and integration level, polymer tacticity, molar mass, and polydispersity. Narrowly dispersed poly(methacrylic acid) (PMAA) with controlled molecular weights and tacticities, as prepared via atom transfer radical polymerization (ATRP),[23] are subjected to the carbodiimide coupling with *n*-octylamine under two extreme conditions: (i) the homogeneous conditions in an organic medium to yield a random octyl distribution (*random* graft amphipol), as verified by ^{1}H and ^{13}C NMR spectroscopic methods, and (ii) the heterogeneous conditions in aqueous micellar media to produce a multiple blocky octyl distribution (*multiblocky* graft amphipol). Both amphipols form well-defined highly stable nanoparticles in aqueous solutions, irrespective of the two synthetic pathways, but the size and molecular weight of the two amphipol self-assemblies are very different, as determined by dynamic as well as static light scattering techniques.

Experimental Section

Materials. Aluminum oxide (90 active, basic for column chromatography) was obtained from Merck and was used as received. Copper(I) bromide (98%) and 1,1,4,7,10,10-hexamethyltriethylenetetramine (HMTETA, 97%) were obtained from Aldrich and were used without purification. Dichloromethane (synthesis grade, >99.8%), *N*-methylpyrrolidone (NMP, 99.5%), and tetrahydrofuran (anhydrous analytical grade, >99.9%) were obtained from Carlo Erba Reactifs SDS. Dicyclohexylcarbodiimide (DCCI, 98%), ethyl 2-bromoisobutyrate (EBIB, 98%), 1-ethyl-3-(dimethylaminopropyl)carbodiimide (EDC, 98%), and trifluoroacetic acid (99%) were obtained from Acros Organics and were used as received. Octylamine (>99%) and sodium dodecyl sulfate (SDS, >99%) were obtained from Fluka. *tert*-Butyl methacrylate (tBMA, 98%, Aldrich) and toluene (anhydrous analytical grade, Carlo Erba Reactifs SDS) were purified by passing through an aluminum oxide column. Triphenylmethyl methacrylate (TPMMA) was prepared and purified according to the literature procedure.[24] Water was deionized with a Millipore Milli-Q Water System.

Polymerizations. Methacrylate-based monomers bearing different protective groups, *tert*-butyl or triphenylmethyl, were polymerized under the same conditions of copper-mediated ATRP to yield the protected PMAA of different tacticities.

Poly(tert-butyl methacrylate) (PtBMA). Copper(I) bromide (10 mg, 0.07 mmol) was added to a 25 mL two-neck round-bottom flask and was degassed by three pump−purge cycles with N_2. tBMA (2 g, 14 mmol), HMTETA (32 mg, 0.14 mmol), and toluene (2.5 mL) were mixed in a 25 mL one-neck round-bottom flask and, after bubbling with N_2 for 30 min, were transferred to the two-neck round-bottom flask via a double-ended needle. The reaction mixture was then heated to 60 °C under N_2 with gentle stirring. EBIB (0.5 g, 2.6 mmol) and toluene (10 mL) were mixed in another 25 mL one-neck round-bottom flask and were purged with N_2 for

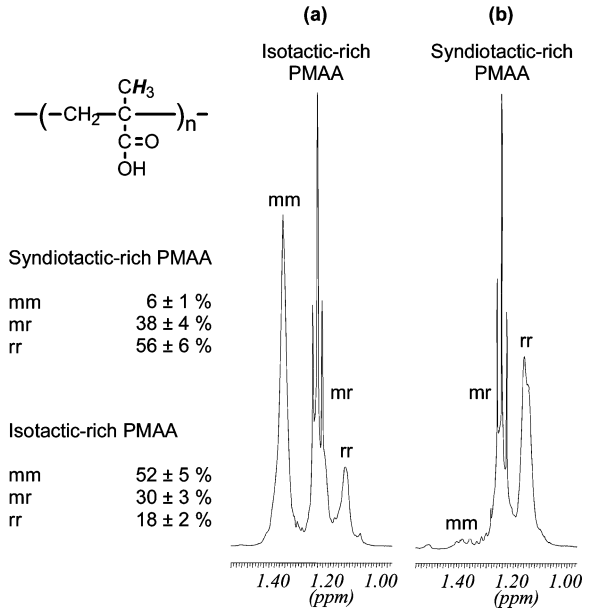

Figure 1. ^{1}H NMR spectra of (a) syndiotactic-rich PMAA and (b) isotactic-rich PMAA in CD_3OD.

30 min. Finally, a small portion of the EBIB initiator solution (0.3 mL) was then added via a microsyringe into the reaction mixture under N_2. After heating for 24 h, the reaction mixture was cooled to room temperature and diluted with THF (10 mL). The crude product was isolated first by adding the diluted reaction mixture slowly into a mixed MeOH/H_2O solvent (80/20 v/v, 400 mL) with vigorous stirring, followed by the vacuum filtration. After drying overnight under reduced pressure, the polymer was purified by column chromatography (Al_2O_3) using THF as the solvent (10 mL) and eluent (100 mL) and was collected by removing the solvent by rotary evaporation at 40 °C. Dissolving in THF (10 mL) and precipitating in a mixed MeOH/H_2O solvent (80/20 v/v, 400 mL) with vigorous stirring yielded the polymer after vacuum filtration and drying under reduced pressure as white solids (1.6 g, 80% yield). The polymer was then characterized by SEC, ^{1}H NMR, and ^{13}C NMR measurements.

Poly(triphenylmethyl methacrylate) (PTPMMA). The polymer was prepared and purified according to the procedure described above, starting from copper(I) bromide (10 mg, 0.07 mmol), TPMMA (4.6 g, 14 mmol), HMTETA (32 mg, 0.14 mmol), toluene (2.5 mL), and EBIB in toluene (0.26 M, 0.3 mL). The polymer was then characterized by SEC, ^{1}H NMR, and ^{13}C NMR measurements.

Hydrolyses. PMAA protected with alkyl groups of different sizes, the *tert*-butyl or triphenylmethyl groups, were all hydrolyzed by using a general procedure of acid-catalyzed hydrolysis.

Syndiotactic-Rich PMAA. In a 100 mL round-bottom flask, PtBMA (2 g, 14 mmol) was dissolved with gentle stirring in CH_2Cl_2 (55 mL) at room temperature. Trifluoroacetic acid (5.4 mL, 70 mmol) was then added into the polymer solution in small portions. The reaction flask was stopped with a glass stopper, and the reaction mixture was stirred for 72 h. After removing the solvent and unreacted trifluoroacetic acid by rotary evaporation at 40 °C, the crude product was first dissolved in methanol (4 mL) and then precipitated in diethyl ether (400 mL) under vigorous stirring. The product was collected by vacuum filtration and was dried under reduced pressure at room temperature overnight to give the white solids (1.2 g, 99% yield). The polymer was then characterized by SEC, ^{1}H NMR, and ^{13}C NMR measurements.

Isotactic-Rich PMAA. The polymer was prepared, purified, and characterized by employing the above-described methods, starting from PTPMMA (4.6 g, 14 mmol), CH_2Cl_2 (55 mL), and trifluoroacetic acid (5.4 mL, 70 mmol).

Hydrophobic Modifications. PMAA was hydrophobically modified under two distinct conditions, in an organic medium (homogeneous conditions) or in an aqueous medium (heterogeneous conditions), to give the amphipols bearing the substituents in a random or multiblocky fashion.

Random Graft Amphipol. PMAA (0.8 g, 9.3 mmol) was dissolved in NMP (10 mL) under stirring at 60 °C in a 100 mL one-neck round-bottom flask. Octylamine (0.24 g, 1.86 mmol) in NMP (5 mL) was added, and the reactants were stirred for 20 min. Then, DCCI (0.44 g, 2.05 mmol) in NMP (2 mL) was added dropwise, and the reaction was kept at 50 °C under stirring for 2 h. After slowly cooling to 0 °C, the reaction mixture was filtered under vacuum, and sodium methoxide in methanol (4 mL, 5 M) was added to the filtrate. The precipitates were collected by vacuum filtration and rinsed with diethyl ether. The crude product was suspended in water, and the impurities were removed by vacuum filtration. The polymer was precipitated by acidification (pH 3, HCl, 1 M) and was collected after centrifugation. The pellet was suspended in water, and the supernatant was removed after centrifugation. The pellet was suspended in aqueous NaOH solution (15 mL, 0.2 M), and the polymer solution was filtered at reduced pressure. The acidification and neutralization of polymer in aqueous solutions were repeated twice, and the pH of the final polymer solution was adjusted to 9. The polymer was then recovered by freeze-drying as white solids (0.75 g, 65% yield) and characterized by ^{1}H and ^{13}C NMR measurements.

Multiblocky Graft Amphipol. In a 25 mL one-neck round-bottom flask, PMAA (0.50 g, 5.8 mmol) was dissolved in an aqueous solution of SDS (16 mL, 0.30 M), followed by the addition of octylamine (0.24 mL, 1.5 mmol). The suspension was gently stirred and warmed to 55 °C. After adjusting the pH of the reaction mixture to 7 with an aqueous NaOH solution (1 M), EDC (0.56 g, 2.9 mmol) was added in one portion and the mixture was stirred for 24 h. The viscous translucent liquid was then cooled to room temperature and mixed well with an aqueous solution of KCl (12 mL, 1 M) to dissolve the polymer and precipitate SDS, which was later removed by centrifugation (5000 rpm, 20 min). The crude product was recovered by acidification (pH 3, HCl, 1 M) and centrifugation (6000 rpm, 30 min) and was rinsed with water. The polymer was repeatedly purified via the KCl suspension, NaOH solubilization−centrifugation, and HCl precipitation−centrifugation cycles to remove most of the remaining SDS, until no precipitation was observed in the NaOH solubilization−centrifugation step. Finally, the white solids were suspended in water, followed by the NaOH solubilization−centrifugation and HCl precipitation−centrifugation steps. Lyophilization of the polymer dissolved in a slightly basic aqueous solution (NaOH, pH 9) gave the polymer as white solids. The polymer contaminated with a small amount of SDS (<5% of the feeding amount) was further purified by extensive dialysis against water and was recovered by freeze-drying. The polymer was then characterized by ^{1}H and ^{13}C NMR measurements.

Size Exclusion Chromatography (SEC) Measurements. SEC results of PtBMA and PTPMMA in THF were obtained on a Viscotek GPCMax VE2001 GPC solvent/sample module that was equipped with a Viscotek model 2501 UV detector and a Viscotek TDA 302 triple detector array. The measured weight-average molecular weight (M_w) was used to evaluate the weight-average degree of polymerization (DP_w) of these protected PMAA, which is also defined as the DP_w of amphipols. SEC measurements of PMAA in aqueous $LiNO_3$ solution (0.5 M) were performed at 40 °C with a Waters 590 programmable solvent delivery system module equipped with a Waters 410 differential refractometer. The measured M_w of the homemade PMAA was used as a reference to estimate the M_w of the commercially available PMAA, which in turn was used to estimate the DP_w of the corresponding amphipols.

Dynamic (DLS) and Static Light Scattering (SLS) Measurements. Simultaneous dynamic and static laser light scattering was made on an ALV/CGS-3 compact goniometer system equipped with an ALV/LSE-5003 light scattering electronic and multiple tau digital correlator and a JDS Uniphase helium−neon laser with an output power of 22 mW, which supplies vertically polarized light with a wavelength of 632.8 nm. The data were collected by monitoring the scattered light intensity at 27 scattering angles (20°−150°) at

Table 1. Chemical and Physical Characteristics of Amphipols

	properties of amphipol precursors (PNaMA)					properties of amphipols		
amphipol	M_w[a]	M_n[a]	M_w/M_n[a]	DP_w[b]	tacticity[c]	degree of C_8H_{17} modification[d] (mol%)	distribution of C_8H_{17}[e]	M_w[f]
AP107-20R	11 600	10 700	1.08	107	75% syndiotactic	20	random	13 500
AP107-20B	11 600	10 700	1.08	107	75% syndiotactic	21	multiblocky	13 600
AP115-20B	12 400	7 300	1.70	115	73% syndiotactic	20	multiblocky	14 500
AP115-30B	12 400	7 300	1.70	115	73% syndiotactic	23	multiblocky	14 800
AP116-20B-I	12 500	10 700	1.17	116	67% isotactic	22	multiblocky	14 800
AP255-20B	27 600	23 200	1.19	255	73% syndiotactic	20	multiblocky	32 100
AP255-30B	27 600	23 200	1.19	255	73% syndiotactic	35	multiblocky	35 500

[a] Determined by SEC measurements in THF of the protected parent chain (PtBMA or TPMMA), except for AP115-20B and AP115-30B which were prepared from the commercially available PMAA and were characterized by SEC measurements in 0.5 M aqueous $LiNO_3$ solution using the parent chain PMAA of AP107-20B as a reference. All values are renormalized to those of the parent chain PMAA in neutralized form (PNaMA). [b] Degree of polymerization estimated from M_w as determined by GPC measurements. [c] Determined by ^1H NMR measurements of PMAA in CD_3OD. [d] Determined by ^{13}C NMR measurements of amphipol in D_2O/CD_3OD (80/20 v/v). [e] Determined by ^{13}C NMR measurements of amphipol in D_2O/CD_3OD (80/20 v/v). [f] Estimated from DP_w of the protected parent chain (PtBMA or TPMMA).

Table 2. Light Scattering Characterization of the Amphipol Micelles in Aqueous Solutions

amphipol	d*n*/d*c*	polymer concn (wt %)	R_h (nm)	R_g (nm)	M_w (g mol^{-1})	$N_{aggregation}$
AP107-20R	0.1713	0.50	3.5	34.5	18 200	1.3
		0.65	3.3	35.4	16 600	1.2
		0.80	3.4	32.3	15 700	1.2
		0.95	3.4	24.4	13 600	1.0
AP107-20B		0.30	12.8	17.2	229 900	17
AP115-20B	0.1756	0.10	8.4	14.6	160 000	11
		0.20	9.6	16.7	164 500	11
		0.30	9.9	19.5	151 100	10
		0.40	8.5	14.8	152 900	11
AP116-20B-I		0.05	14.6	15.8	308 600	21
		0.10	15.1	11.4	273 200	19
		0.50	15.8	13.5	223 700	16
AP255-20B		0.10	20.8	37.1	539 600	17
AP255-30B		0.05	60.1	74.4	6 993 000	218
		0.10	60.7	87.4	6 666 700	208

25 °C. Temperature control within 0.1 °C was achieved using a Julabo F25 refrigerated bath circulator, and measurements were performed using polymer solutions filtered through membranes of 0.20 μm pore size directly into scintillation vials of 1.0 cm diameter prior to measurements. Data were analyzed using the ALV-Correlator Software Version 3.0 and ALV-Fit & Plot Software provided by the manufacturer.

Refractive Index Measurements. The d*n*/d*c* values of amphipols were obtained from the refractive index of aqueous polymer solutions measured at various concentrations at ambient temperature, with a Thermo Finnigan Spectrasystem RI-150 refractive index detector.

Sample Preparation. Stock solutions of amphipols were prepared by dissolving the polymer in water and were diluted later with water to the desired concentration for RI measurements. Samples for NMR measurements were obtained by first dissolving the polymer in D_2O and then diluting the solution with CD_3OD to a final D_2O/CD_3OD mixing ratio of 20/80 (v/v). Aqueous solutions of amphipols and of SDS for DLS and SLS measurements were prepared by directly dissolving the polymer or surfactant in 0.1 M aqueous NaCl solution. To prepare the amphipol/SDS mixtures, a fixed volume of the amphipol stock solution was combined with various amounts of the SDS stock solution and finally diluted with aqueous NaCl solution to a fixed final volume. All solutions were gently mixed to ensure a complete dissolution of the polymers or of the surfactant as well as to avoid foaming and were prepared at least 24 h before use and/or in advance of measurements to ensure that equilibrium was reached.

Results

Amphipol Synthesis and Characterization. The synthesis of a new series of amphipols, which are poly(methacrylic acid)s (PMAA) modified with moderate amounts of octyl side chains, is summarized in Scheme 1. The general synthetic route involves (i) the preparation of narrowly dispersed PMAA via atom transfer radical polymerization (ATRP), which controls the polymer molar mass and tacticity, and (ii) the coupling reaction of PMAA with *n*-octylamine under the conditions that regulate the hydrophobe distribution along the polymer main chain. In this section, we describe at first the synthesis of PMAA parent chains of different tacticities, though prepared under similar ATRP conditions, using two bulky monomers that afford predominantly isotactic or syndiotactic polymer chains. We then describe in the second part the hydrophobic modification of these PMAA parent chains under dissimilar conditions that yield amphipols with a random or multiblocky hydrophobe distribution.

Synthesis of PMMA. By using copper(I) bromide and 1,1,4,7,-10,10-hexamethyltriethylene tetramine as a catalyst system and ethyl bromoisobutyrate as an initiator, polymerization of *tert*-butyl methacrylate (tBMA) in toluene at 60 °C gave the poly(*tert*-butyl methacrylate) (PtBMA) in 24 h, with a monomer conversion ranged from 80% to 85%. All PtBMA have a narrow molecular weight distribution ($M_w/M_n < 1.2$) and a molecular weight well-agreed with that predetermined by the feeding monomer-to-initiator ratio. In one case, PtBMA with a weight-average molecular weight (M_w) as high as 36 200 g mol^{-1} is obtained, while retaining a low polymer polydispersity ($M_w/M_n = 1.19$). In another case, polydispersity index as low as 1.08 is determined for a PtBMA ($M_w = 15\,200$ g mol^{-1}) prepared under similar ATRP conditions. The polymer composition and structure are confirmed from the ^1H NMR spectra of PtBMA in $CDCl_3$ (supplemental Figure 1 in Supporting Information), which presents a sharp singlet at δ 1.41 ppm due to the methyl protons of the *tert*-butyl groups. Also, the ratio of integrals of the signals assigned to the methyl groups of diverse spacial arrangements along the polymer main chain,[25]

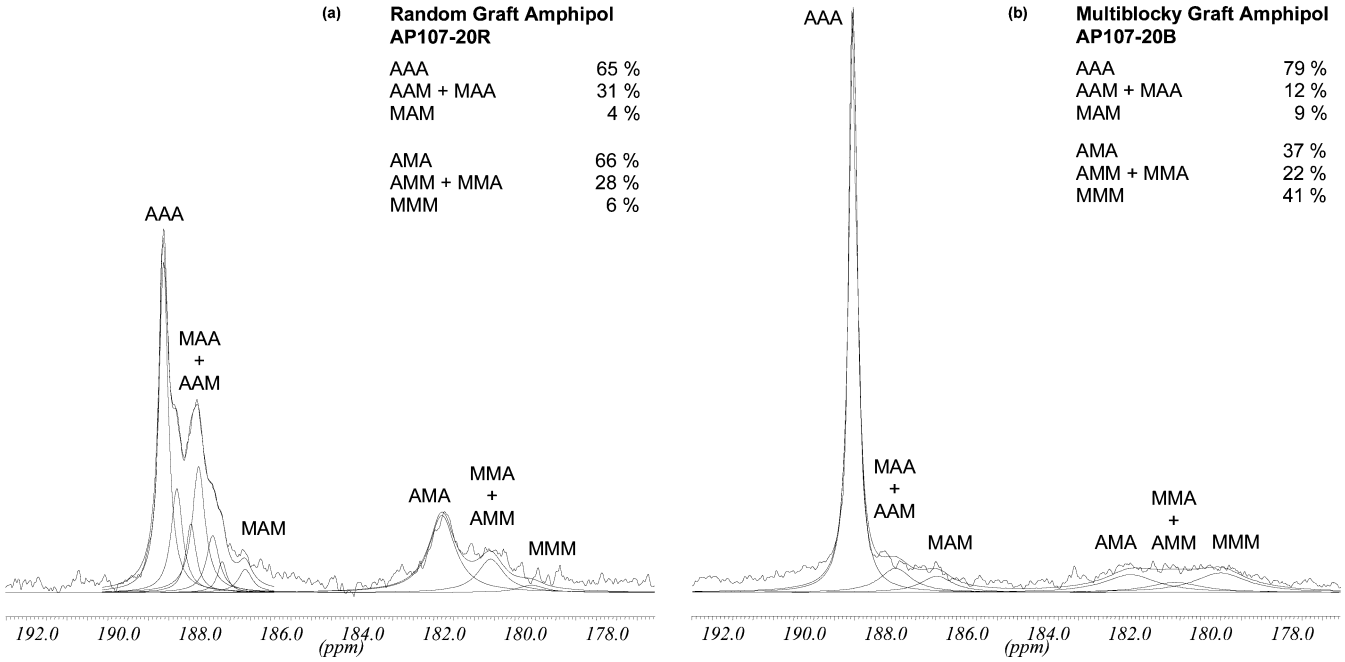

Figure 2. ^{13}C NMR spectra of (a) AP107-20R and (b) AP107-20B in CD_3OD/D_2O (20/80 v/v).

centered at δ 1.25, 1.11, and 1.03 ppm representing accordingly the isotactic (mm), heterotactic (rm), and syndiotactic (rr) triads, clearly shows a preference for syndiotacticity (mm:rm:rr = 9:36:55). Deprotection of PtBMA with excess trifluoroacetic acid in dichloromethane at ambient temperature yielded the syndiotactic-rich PMAA in quantitative yields. The polymer tacticity is confirmed from the ^1H NMR measurements of PMAA in CD_3OD (Figure 1). The methyl proton signals due to the three triads at δ 1.31, 1.18, and 1.10 ppm show the same syndiotacticity as before hydrolysis (mm:rm:rr = 6:38:56). When using the methacrylate monomer bearing a protective group with increased bulkiness, triphenylmethyl methacrylate (TPMMA), on the other hand, a well-defined poly(triphenylmethyl methacrylate) (PTPMMA, M_w = 38 200 g mol^{-1}, M_w/M_n = 1.17) of notably enhanced isotacticity (mm:mr:rr = 52:30:18) is obtained by the copper-catalyzed ATRP under similar conditions (Figure 1).[26] These results clearly imply that the well-controlled copper-mediated ATRP reported in here provides a simple route to narrowly dispersed isotactic-rich or syndiotactic-rich PMAA. Also used in this work is a commercially available syndiotactic-rich PMMA (mm:rm:rr = 8:38:54, M_w = 12 400 g mol^{-1}) with a weight-average degree of polymerization (DP_w) similar to that of the homemade PMAA ($\sim$110) but with an increased polydispersity index (M_w/M_n = 1.70). The physical characteristics of all PMAA used (in neutralized form, poly(sodium methacrylate), PNaMA) for the amphipol preparation are listed in Table 1.

Hydrophobic Modification of PMMA. Amphipol AP107-20R is prepared from PNaMA (M_w = 11 600 g mol^{-1}, M_w/M_n = 1.08, DP_w = 107) via the coupling reaction with *n*-octylamine in *N*-methylpyrrolidone, using *N*,*N*′-dicyclohexylcarbodiimide as the coupling agent. The incorporation level and distribution sequence of octyl side chains grafted to PNaMA are determined by ^1H and ^{13}C NMR measurements of the amphipol in a mixed CD_3OD/D_2O solvent (80/20 v/v). The chemical grafting of octyl side chains via the amide linkage formation is confirmed from the ^1H NMR spectra (Figure 2 of Supporting Information), showing an isolated signal at δ 3.06 ppm attributed to the proton resonance of methylene group linked to the amide nitrogen. This signal, as well as the signals due to other methylene and in particular the methyl protons of octyl side chains, appeared however as broad signals when using solely D_2O as the solvent, even though the amphipol is readily soluble in D_2O and aqueous solutions. Such signal broadening and loss of resolution indicate a high restriction in the motions of these hydrophobic octyl side chains in D_2O, suggesting the associations of hydrophobes to form hydrophobic nanodomains and the formation of micelle-like self-assemblies of amphipol (see below).[27] The random distribution of octyl groups along the poly(sodium methacrylate) backbone is evidenced by the resonance of carbonyl carbons of the sodium methacrylate units (Figure 2). The resolved signals reveal that most of the sodium methacrylate units are each located between two sodium methacrylate units in an AAA triad, appearing as a fairly sharp and intense signal at δ 188.5 ppm,[28] with a small portion of these units each being located between a sodium methacrylate unit and an octyl methacrylamide unit (AAM and MAA triads, δ 187.6 ppm). Also, the peak attributed to the MAM triad appears as an extremely weak signal at δ 186.6 ppm. The ratio of the contributions of each triad matched well with a random Bernoullian statistics (Figure 2a).[28] A parallel result is obtained from the carbonyl carbon resonance of the octyl methacrylamide units, indicating that no considerable amount of these units being existed as a MMM triad (δ 179.7 ppm). Instead, these octyl methacrylamide units are mostly distributed in an AMA triad (δ 181.6 ppm, 66%) and partly in the MMA and AMM triads (δ 180.7 ppm, 28%). These results strongly support that the octyl groups of amphipol AP107-20R are existed mainly as isolated methacrylamide units, which are individually well separated by short segments of a few sodium methacrylate units and to a lesser extend as isolated pairs of methacrylamide units.

In contrast, similar coupling reaction of the same parent PNaMA (M_w = 11 600 g mol^{-1}, M_w/M_n = 1.08) but performed in an aqueous micellar solution of sodium dodecyl sulfate (SDS) produces an amphipol that carries the octyl side chains in a multiblocky fashion. As illustrated with the ^{13}C NMR spectrum of AP107-20B in Figure 2b, the carbonyl carbon signals appeared predominantly at δ 188.5 ppm, due to the AAA triad of the sodium methacrylate units, which is enhanced notably as compared to the ^{13}C NMR spectrum of AP107-20R. This

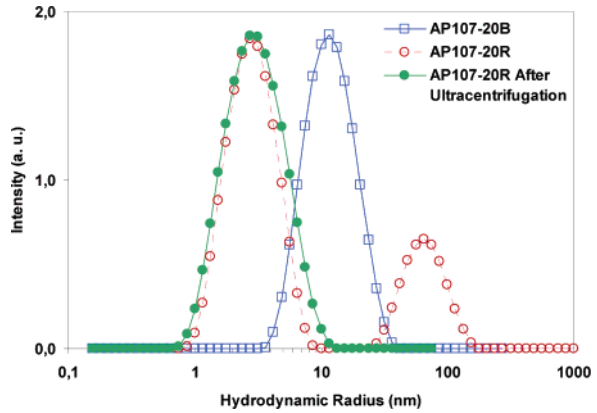

Figure 3. Hydrodynamic radius distribution of AP107-20B (0.30 wt %) and AP107-20R (0.95 wt %) in 0.1 M aqueous NaCl solutions. "Ultracentrifugation" stands for one sample centrifuged at 200 000*g* for 80 min to remove the contribution of large particles.

enhancement clearly implies that the blocks of sodium methacrylate units are lengthened considerably, and the separation among individual octyl methacrylamide unit is reduced accordingly. Supporting evidence also includes the carbonyl carbon signal of the octyl methacrylamide units which appeared mainly at δ 181.6 ppm (MMM triad), confirming that a large number of octyl groups of the amphipol AP107-20R exist as blocks of closely spaced side chains, which are separated by long blocks of sodium methacrylate units to give an overall multiblocky polymer structure.

Since both amphipols AP107-20B and AP107-20R have the same hydrophobe grafting degree (20.2 ± 0.6 mol %) and are prepared from the same parent PMAA, the differences seen on the spectroscopic data are undoubtedly attributed to their distinct polymer microstructures, arising from the diverse conditions of polymer modification. The diimide-mediated coupling reaction under the homogeneous conditions, at which all the reactants are well solubilized in the reaction mixtures, is widely used to obtain amphiphilic polymers randomly grafted with hydrophobes.[29] Thus, the modification of PMAA in an organic medium (homogeneous conditions) leads to a random hydrophobe distribution (random graft amphipol). Parallel coupling reaction in aqueous media, however, is proceeded under the heterogeneous conditions. Because of the very low solubility of *n*-octylamine in water (0.2 g L^{-1}), the octylamine molecules are not individually distributed in the aqueous phase but are associated with the SDS molecules to form mixed micelles that act as the nanoscaled reactors.[30] Such octylamine integration into the SDS micellar structures markedly suppresses the randomness of the hydrophobic modification, in which case the octylamine molecules are coupled in groups with PMAA. As the water-soluble EDC was 2-fold in excess with respect to the water-insoluble octylamine, the grafting process should be predominantly controlled by the amount and distribution of octylamine within the mixed micellar structure, but not by the randomness and number of active sites on the reactive intermediate formed from PMAA and EDC prior to the coupling with octylamine. Once the activated acid intermediate is formed in the aqueous phase, the amino groups of octylamine molecules localized on the micelle surface react to yield the PMAA grafted with octyl groups in a multiblocky manner (multiblocky graft amphipol).

By following the same synthetic route (under heterogeneous conditions), five more multiblocky graft amphipols were prepared from three PNaMA with distinct microstructures. Modified at the same grafting degree (20.7 ± 0.9 mol %) as AP107-20B are the PNaMA of increased polydispersity (M_w/M_n = 1.70, AP115-20B), of enhanced isotacticity (mm = 52%, AP116-20B-I), and of increased molecular weight (M_w = 27 600 g mol^{-1}, M_w/M_n = 1.19, AP255-20B). Another two amphipols were synthesized under similar heterogeneous conditions but with a higher grafting degree (30 mol %) from the polydisperse PNaMA (M_w/M_n = 1.70, AP115-30B) and from the PNaMA of increased molecular weight (M_w = 27 600 g mol^{-1}, M_w/M_n = 1.19, AP255-30B). Note that amphiphilic multiblock copolymers, with a hydrophobe distribution sequence quite similar to that of the multiblocky graft amphipols reported in here, have been prepared by various copolymerization methods: (i) template copolymerization of hydrophilic monomers and hydrophobic monomers in the presence of a polymer,[31] (ii) micellar copolymerization of hydrophilic monomers and hydrophobic monomers in aqueous surfactant solutions,[32] and (iii) copolymerization of hydrophilic monomers and surfactant-like amphiphilic monomers in water.[33] In many cases, high molar mass amphiphilic multiblock copolymers are obtained with low hydrophobe incorporation levels (<5 mol %). The above-described postpolymerization polymer modification approach, moreover, permits the synthesis of series of amphiphilic copolymers that possess certain identical molecular characteristics as preserved from the parent polymer.

Self-Assembly of Amphipols. All seven amphipols are soluble in water and in aqueous salt solutions, at a concentration depending on the polymer chemical composition and microstructure. The multiblocky graft amphipol bearing 30 mol % of octyl groups, AP115-30B, for instance, swelled slowly at a polymer concentration of 1.0 g L^{-1} in 0.1 M aqueous NaCl solution and resulted in a highly stable homogeneous turbid aqueous suspension. A clear solution is obtained when lowering the polymer concentration to 0.3 g L^{-1}, but the scattering intensity at this low concentration remains high (7-fold as compared to toluene at 90°), hinting at the formation of large aggregates in the polymer solutions. The solubility and scattering intensity of the corresponding solutions are enhanced for the amphipol of similar grafting level but with an increased polymer molecular weight, (AP255-30B, 0.5 g L^{-1}, 31-fold as compared to toluene at 90°), which also forms a stable homogeneous turbid aqueous suspension at an increased polymer concentration of 5.0 g L^{-1}. With a hydrophobe grafting level of 20 mol %, the three amphipols of a comparable molar mass (AP107-20B, AP115-20B, and AP116-20B-I) are all soluble within the tested concentration range (0.1−5.0 g L^{-1}), but the polymer solutions exhibit a significant reduction in the scattering intensity (1.0 g L^{-1}, 3−5-fold as compared to toluene at 90°). This solution scattering intensity is reduced further in the case of the readily water-soluble random graft amphipol AP107-20R. Even at a concentration as high as 10 g L^{-1}, the solution scattering intensity remains low (4-fold as compared to toluene at 90°), and no visible enhancement is observed in the solution viscosity, suggesting the formation of small aggregates in aqueous solutions. Although the amphipols bearing different polymer microstructures and chemical compositions all form clear solutions in aqueous media, the large differences in the intensity of scattered light determined for these solutions are clear signs of distinct nanosized aggregate formations. Results from dynamic (DLS) and static light scattering (SLS) measurements revealed that all amphipols form nanoparticles in aqueous solutions, and the size and number of associated polymers of the amphipol self-assemblies are strong functions of the polymer molecular characteristics like molar mass, polydispersity, tac-

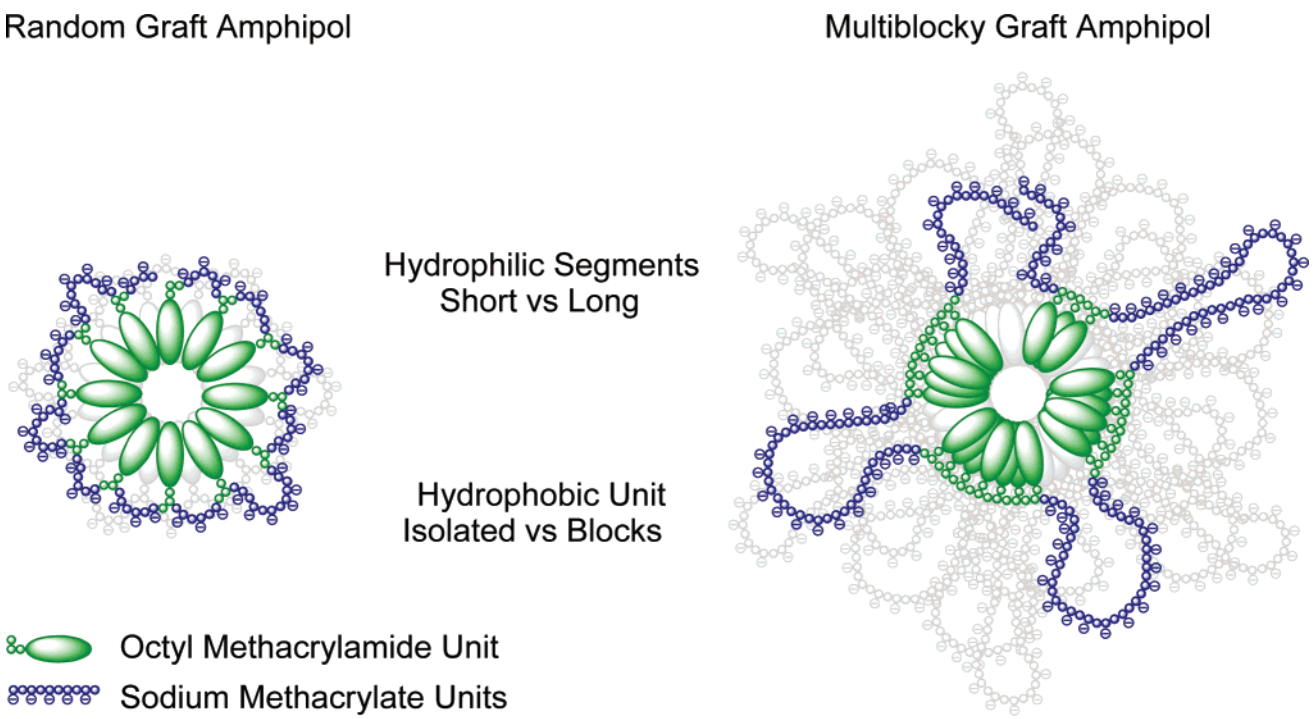

Figure 4. Conceptual representation of the amphipol self-assemblies.

ticity, and, in particular, the distribution sequence of octyl side chains.

Effects of Hydrophobe Distribution. Figure 3 presents the hydrodynamic radius distribution for the random graft amphipol AP107-20R in aqueous NaCl solution (0.1 M). At a polymer concentration as high as 9.5 g L^{-1}, the amphipol exhibits a preferential formation of small nanoparticles with a mean Stokes radius of 3.1 nm, with the presence of a small amount of large aggregates (~70 nm). Varying the polymer concentration (1.0−9.5 g L^{-1}) has no major influence on either the dominant formation of small nanoparticles or the average hydrodynamic radius of these small nanoparticles (3.5 ± 0.5 nm), except the mean radius of the large aggregates is varying between 70 and 100 nm (Table 2). Furthermore, the small nanoparticles remain in the solution under the conditions of ultracentrifugation (~200 000*g*, 20 °C, 80 min), whereas the large aggregates essentially precipitated (Figure 3). The absence of sedimentation of these nanoparticles was confirmed by comparing the fraction of scattered light intensities due to the small nanoparticles before and after ultracentrifugation. These nanoparticles are stable for weeks, showing no important change in the size and size distribution, or the solution scattered light intensity. Furthermore, the large aggregates do not reappear even after allowing the solution of small nanoparticles to stand for a prolonged period. Evidently, these large aggregates did not originate from the small nanoparticles. Data from SLS measurements suggest that each small nanoparticle is on average composed of one polymer chain (Table 2). The weight-average molecular weight of the small nanoparticles (M_w = 13 600−18 200 g mol^{-1}), as determined by data extrapolation to zero scattering angle at each polymer concentration, is more or less the molecular weight of amphipol AP107-20R (13 500 g mol^{-1}), as estimated from the weight-average molecular weight of the parent PNaMA (M_w = 11 600 g mol^{-1}). Also shown in Figure 3 is the hydrodynamic radius distribution for the multiblocky graft amphipol AP107-20B in aqueous NaCl solution (0.1 M). Parallel to the random graft amphipol AP107-20R, this amphipol self-assembles and forms stable nanoparticles in aqueous solutions, and neither extensive ultracentrifugation nor prolonged standing influences the polymer concentration-independent formation of nanoparticles. On the contrary, these nanoparticles exhibit only a single size distribution (unimodal population) with a mean radius of 12.8 nm and a weight-average molecular weight of 229 900 g mol^{-1}, which corresponds to an average aggregation number of 17 polymer chains in each nanoparticle.

Given that the amphipols AP107-20R and AP107-20B are prepared from the same parent PNaMA (M_w = 11 600 g mol^{-1}, M_w/M_n = 1.08) and have the same hydrophobic modification level (20.2 ± 0.6 mol %), the vast differences in the amphipol self-assembly are therefore mainly due to the hydrophobic modification method, which ultimately controls the polymer microstructure. The amphipol AP107-20R has a microstructure resembling that of polysoaps (Figure 4), with a relatively short hydrophilic spacer (~4 sodium acrylate units) between every two hydrophobic tails. In aqueous solutions, the octyl groups associate to form a hydrophobic core that presumably shares many properties with spherical surfactant micelles. Alternatively, in the multiblocky graft amphipol AP107-20B, the octyl groups are closely spaced along the poly(sodium methacrylate) backbone, and the amphipol AP107-20B has a microstructure resembling that of multiblock copolymers (Figure 4), carrying hydrophobic groups widely separated with long hydrophilic spacers. As the short segments of octyl methacrylamide of the multiblocky graft amphipol AP107-20B undergoes self-association in aqueous solutions, the long segments of sodium methacrylate that form the nanoparticle corona are seemingly less effective on covering uniformly the hydrophobic globule and on shielding from interpolymeric associations (see Discussion).

Effects of Polymer Molar Mass, Polydispersity, and Tacticity. Three additional parameters of polymer microstructure are considered by using structurally different amphipols bearing a fixed integration level of hydrophobes (~20 mol %). Compared to the distribution sequence of octyl side chains, the structural parameters including polydispersity, tacticity, and degree of polymerization of the parent poly(sodium methacrylate) main chain have less influences on the formation of amphipol self-aggregates in aqueous solutions (Table 2). As AP255-20B is

Table 3. Salt Effect on the Amphipol Self-Assembly in Aqueous Solutions

amphipol	solvent	R_h (nm)	R_g (nm)	M_w (g mol^{-1})	$N_{aggregation}$
AP107-20B	0.05 M NaCl	11.5			
	0.10 M NaCl	11.1			
	0.25 M NaCl	11.0	16.8	217 100	16
	0.50 M NaCl	11.2			
	1.00 M NaCl	11.8	16.7	228 600	17
	2.50 M NaCl	13.7	19.8	245 000	18
AP255-20B	0.02 M NaCl	36.8	38.6	584 700	18
	0.10 M NaCl	20.8	35.1	585 000	18
	0.02 M KCl	35.5	36.8	546 700	17
	0.10 M KCl	21.6	34.9	511 200	16

the structural analog of AP107-20B, increasing the polymer chain length ($DP_w = 255$ vs 107) increases the size but not the number of associated polymers chains per self-aggregate. Significant polymer molar mass distribution broadening reduces only slightly the Stokes radius and the weight-average molecular weight of the amphipol self-aggregates (AP107-20B vs AP115-20B). In this case (broadly dispersed AP115-20B), the increased portion of low molecular weight polymer chains may balance the effect of longer chains, which increase the size of self-aggregates. Similarly, enhancing the polymer isotacticity (mm:rm:rr = 52:30:18 vs 7:38:56) has little effect on the size and the number of associated polymers, as in the case of amphipol AP116-20B-I (vs AP107-20B). As compared to the syndiotactic-rich amphipol AP107-20B, the isotactic-rich amphipol AP116-20B-I shows an averaged 20% increase in the hydrodynamic radius of the self-aggregates formed but exhibits no parallel increase in the number of associated polymers, hinting at the formation of amphipol self-aggregates that possess an expanded structure. This result is consistent to the behavior of poly(alkyl methacrylates), in which case stronger cohesive interactions are observed for the syndiotactic polymers than for the isotactic ones.[34] As listed in Table 2, when considering the three multiblocky graft amphipols that are prepared from PMAA of low polydispersities and modified with 20 mol % of hydrophobes (AP107-20B, AP116-20B-I, and AP255-20B), nanoparticles are formed in aqueous media from a roughly constant number of polymer chains (19 ± 2), regardless of the vast differences in their microstructure. This consistency clearly points toward the predominant impact of hydrophobe distribution sequence that determines the intrinsic hydrophilic/hydrophobic balance of the amphipols, which in turn controls the amphipol self-assembly in aqueous solutions. The chain length modulates however the molecular weight of self-assemblies that formed from amphipols of well-defined lengths and low polydispersity, as suggested by the roughly constant number of chains per aggregate.

Stability of Amphipol Self-Assemblies. The unique formation of amphipol self-aggregates is verified by its independence of the polymer solution preparation procedure. The well-defined nanoparticles are formed from amphipols by directly dissolving either the polymer in aqueous salt solution or the polymer and salt simultaneously in water. The same nanoparticles are also obtained when diluting either the salt-free aqueous polymer solution with aqueous salt solution or the aqueous salt solution of amphipol with water. In addition, our results suggest the high stability of amphipol self-assemblies in aqueous solutions of varying ionic strengths. Indeed, the number of aggregated polymer chains and hydrodynamic radius of these self-aggregates formed from amphipol AP107-20B, for example, are essentially invariant with salt concentration (17 ± 1 and 11.4 ± 0.4 nm, respectively), as the NaCl concentration is increased 50 times from 0.05 to 2.5 M (Table 3). In the case of the high molecular weight analogue AP255-20B at low NaCl concentrations, the number of associated polymer chains remains constant while the hydrodynamic radius is reduced by less than half with increasing ionic strength by a factor of 5 (Figure 5). Parallel results are obtained when using KCl instead of NaCl (Table 3). These features thus imply a significant expansion of the negatively charged corona of the amphipol self-aggregates at low ionic strengths. Reducing the amount of ionized salt weakens its screening effect on the carboxylate groups, which then strengthens the repulsive interactions and extends the sodium methacrylate segments in the corona. At low ionic strengths and with an expended corona, R_g/R_h nears a value of 1.2, which is indicative of a globular nature of the micellar structures. At a higher ionic strength, the high R_g/R_h value (∼2) suggests some elongation of the micellar structures, whose ellipticity could be masked at low ionic strengths by the swelling of ionic corona.

Amphipol−SDS Interactions. The well-controlled self-assembly of amphipols in aqueous solutions is finally examined with the presence of the surfactant sodium dodecyl sulfate (SDS). We check here the stability of polymer self-associates, that is, the resistance toward fragmentation by a surfactant, which is classically recognized as a strong solubilizing agent. The self-aggregates of AP107-20B are analyzed at a fixed polymer concentration (0.1 g L^{-1}) upon mixing with an increasing amount of SDS (0.2−2.0 mM). The scattered light intensity of the mixed amphipol/SDS solutions and hydrodynamic radius of the nanoparticles are plotted as a function of SDS concentration. As evident in Figure 6, the added SDS has very little effect on the formation of amphipol self-assemblies at any concentration of SDS far below its critical micelle concentration (cmc, 1.4 mM in 0.1 M NaCl). The hydrodynamic radius of these nanoparticles is unchanged (11.6 ± 0.1 nm), up to a SDS concentration of 0.8 mM. Within the SDS concentration ranged from 1.0 to 1.4 mM, there exists a small but continuous decrease in both the scattered light intensity and the hydrodynamic radius. Further addition of SDS results in the formation of self-assemblies with an essentially lower but constant hydrodynamic radius (7.4 ± 0.4 nm), in the SDS concentration window of 1.6−2.0 mM. Since the amphipol and SDS are both negatively charged, the observed variations are clear implications of the considerable hydrophobic interactions between the polymer and surfactant.[35] Also accompanied by the reduction in scattered light intensity and hydrodynamic radius is the substantial drop in the molecular weight of these nanoparticles and accordingly the fragmentation of the initial polymer self-assemblies. It is not surprising to see the formation of a mixed micellar structure via the incorporation of SDS molecules into the amphipol nanoparticles, which favors the formation of micelles whose size gradually become close to the size of SDS micelles. The important conclusions here are that both the size and molecular weight of polymer self-assemblies are not significantly affected by the surfactant at SDS concentrations below the cmc, but the polymer self-

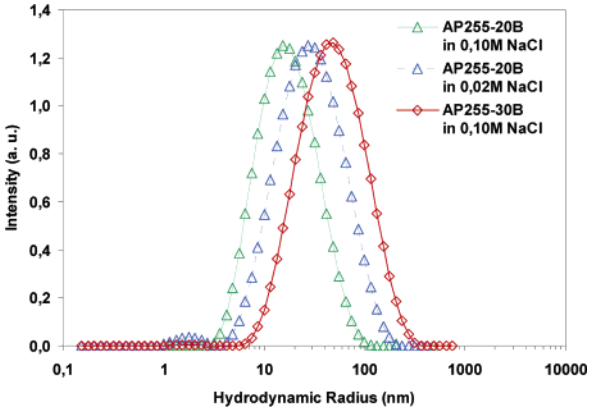

Figure 5. Hydrodynamic radius distribution of AP255-20B (0.10 wt %) and AP255-30B (0.10 wt %) in aqueous NaCl solutions.

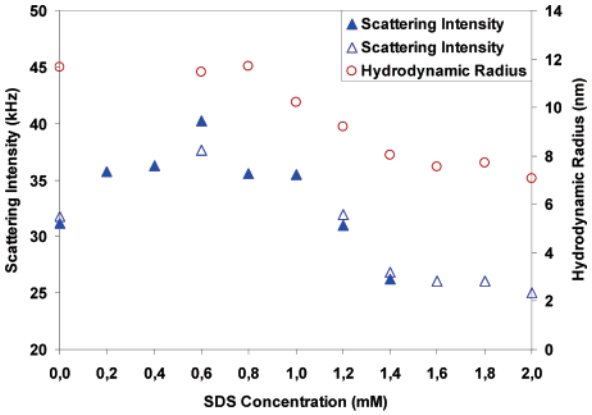

Figure 6. Changes in the hydrodynamic radius and scattered light intensity for 0.1 M aqueous NaCl solutions of AP107-20B (0.1 g L^{-1}) as a function of SDS concentration: 0.2−1.4 mM (filled triangles) and 0.6−2.0 mM (empty triangles).

associates can be moderately dissociated at SDS concentrations above the cmc.

Discussion

Consequences for Applications in Amphiphilic Polymer Thickeners. Copolymerization in water[28] or in spherical micelles[18] is known to produce amphiphilic copolymers containing short hydrophobic blocks, with enhanced associating properties including the formation of physical gels with high moduli. The concentration range used for these gelations involving enhanced interchain associates (semidilute regime) is considerably higher than those studied in the present work. The reports of large aggregates in gels of block copolymers refer accordingly to the networks of long polymer chains connected by small micelle-like clusters. Controlling the parameters that affect the compactness and size of the micellar interchain assemblies should enable one to control the mechanical properties of these gels. The structure of the corresponding clusters (i.e., the transient cross-links) is often largely unknown. Our data suggest that on a nanometer scale the organization of compact and monodispersed clusters is preserved irrespective of the blockiness, but the number of chains (functionality of the cross-links) in a cluster may increase significantly. The knowledge of size and in the future of lifetime and stability of these well-organized clusters should help the development of amphiphilic polymer-based thickeners with exquisite adjustable and controllable properties.

Consequences for Applications in Biology (Amphipols). Short amphiphilic polymers have found applications in biology to encapsulate in micelle-like complexes small hydrophobic colloids, including membrane proteins and quantum dots.[22,36] Several issues need to be addressed concerning the proper handling of these amphipols in biological applications. Of primary importance for the structural analysis of proteins and the use of probes such as quantum dots trapped in amphipol is the fact that these objects need to remain small and monodisperse in size. We observed that the amphipols with a blocky hydrophobe distribution did not form objects polydisperse in size even by simple solubilization in water, though their micelle-like assemblies have significantly higher molecular weights as compared to those formed from the random copolymers. It is interesting to note that these features are shared by polymers of markedly different polydispersity in length, which points to the primary importance of the random hydrophobe distribution in the formation of aggregates. The aggregates formed by random copolymers can however be removed by ultracentrifugation, if need be, and did not re-form afterward in the purified solution that contained the monodisperse complexes with radii less than 5 nm. The control of hydrophobe distribution sequence, especially random vs multiblocky as reported in here, thus finally offers the possibility to achieve monodisperse assemblies as either small and presumably spherical particles or large and most likely elongated ones (Figure 7).

Controlled Self-Assemblies of Multiblocky Graft Amphipols (Absence of Large Aggregates). Various theoretical approaches, as developed by Dobrynin, Rubinstein, Borisov, and Halperin, predict the formation of well-defined self-assemblies from amphiphilic polyelectrolytes that comprised of a repeated sequence, with a hydrophilic chain and a hydrophobic unit. The balance among the elastic energy of polymer chains, the electrostatic and steric repulsions among monomer units, and the energy of water/hydrophobe interface results in a well-defined nanostructures.[37] Although the random hydrophobe distribution and the polydispersity of our synthetic macromolecules could hamper the self-organization of the polymer amphiphilic moieties, we achieved in practice a well-defined polymer self-organization. The polydispersity of amphipols may be averaged by the clustering of several chains in the self-associates. It appears however to be difficult to predict how the size of the assemblies should be affected by enhancing the blockiness, that is, when the hydrophobic side chains are grouped as short blocks while maintaining the fraction of hydrophobic monomers constant in the polymer chain.

Following the authors cited above, the parameter controlling the growth of self-assemblies (and accordingly elongation) compares the size of hydrophobes with the length of hydrophilic chain between adjacent hydrophobic groups. Enhancing the hydrophobe blockiness lengthens the hydrophilic chain separating adjacent hydrophobes, which then should favor the formation of small (spherical) self-assemblies. In practice, however, short or isolated hydrophobic groups may not be hydrophobic enough to cluster into the hydrophobic core, and therefore they belong to the chain segments quoted as hydrophilic. The fraction of hydrophobic groups that do not enter into the clusters can be as high as 50 mol % for random copolymers of low modification degrees.[38] On the basis of the conformation entropy of the chains, it has been shown that groups of hydrophobic moieties (at a fixed degree of modification of the chain) show strong enhancement of intrachain associations.[39] This phenomenon increases the volume of micellar core of the blocky chains as compared to that of the random ones, which in turn favors the elongation. In addition, the contribution of Coulombic repulsions to the free energy of self-assembling may also lead to subtleties if the degree of ionization of the chain depends on clustering[37]

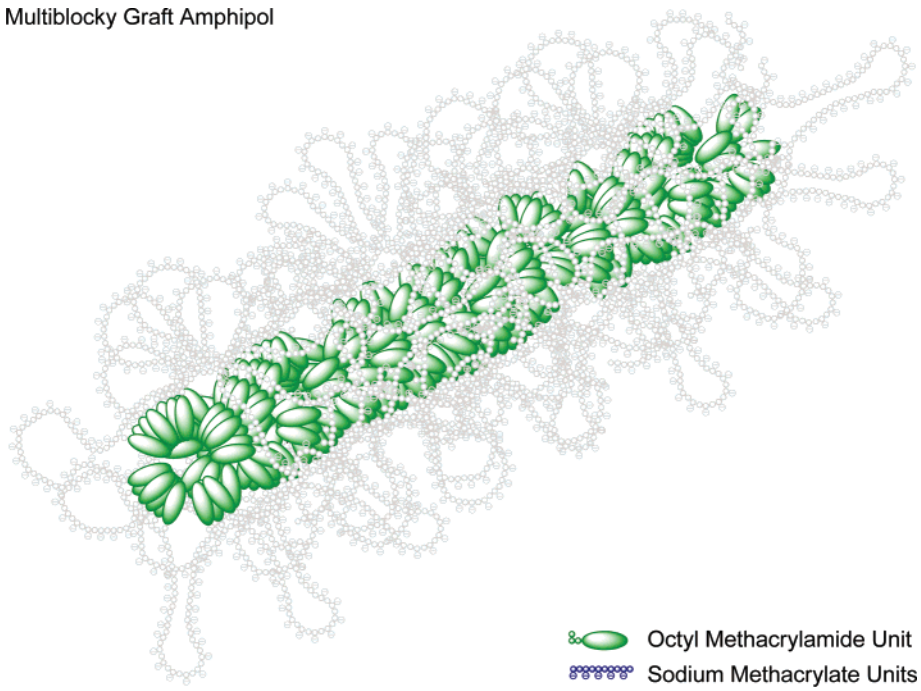

Figure 7. Conceptual representation of the elongated self-assembled structure of multiblocky graft amphipols.

or if the polyelectrolytes loops are longer than the Debye length (screening of Coulombic repulsions among the hydrophilic segments).

We obtained that enhancing the blockiness leads to an elongation and growth of the clusters of polymer chains. The enhanced contribution of hydrophobes distributed in a multiblocky fashion to the micellar cores presumably counteracts the simple geometric effect based on the elongation (multiblocky vs random distribution) of hydrophilic poly(sodium methacrylate) loops between two adjacent hydrophobic segments. In addition, the longest hydrophilic loops may have a negligible effect on the shape of the clusters due to the screening of interloop Coulombic repulsions. In this case, it is not surprising that amphipols with enhanced blockiness show weaker aggregation in solutions (i.e., less particles with radii beyond 40 nm) than the random ones. The length of the purely hydrophilic regions is shorter than the Debye length in the case of random copolymers, and the (random) fluctuation of this length accordingly affects the nanoparticle formation. At a modification degree of ~20 mol %, the average number of anionic monomers between adjacent octyl groups (~4) fluctuates at random by a factor as large as ±2. The presence in solution of a minor fraction (0.1 wt %) of aggregates with a largely increased hydrodynamic radius (~50−70 nm) could be attributed to such fluctuation of the density of octyl side chains for the random copolymers.

Conclusions

Dynamic and static light scattering experiments provide strong evidence that amphipols composed of a poly(sodium methacrylate) main chain and a moderate level of octyl side chains self-assemble to form distinct micelle-like nanoparticles, exhibiting the important role of hydrophobe distribution sequence in the polymer structure−property relationship. While the random graft amphipol predominantly associates intramolecularly as aggregates from one or two chains, the multiblocky graft amphipol associates intermolecularly as well-defined multiple polymer chain aggregates. A direct comparison between these two amphipols is made possible by the postpolymerization hydrophobic modification of a single parent polymer under either the homogeneous or heterogeneous conditions, which controls the distribution of hydrophobes and, more importantly, produces hydrophobically modified polymers with the same degree of polymerization, polydispersity, and tacticity. Modifying solely the hydrophobe distribution sequence promotes the interpolymeric hydrophobic associations and transforms the morphology of amphipol self-aggregates possibly from a spherical to an elongated micellar structure. Controlling the self-assembly of amphiphilic polymers is an important issue, particularly when designing these polymers for applications such as the incorporation or complexation with small molecules or macromolecules that often possess widely different structural characteristics.

Acknowledgment. We thank C. Ebel and F. Vial for helpful discussion on the size and shape of nanoassemblies and M. N. Rager for NMR spectra. The work was supported by CNRS (Liu's Grant).

Supporting Information Available: ^{1}H NMR spectra of the parent poly(*tert*-butyl methacrylate) and of the random graft amphipol AP107-20R. This material is available free of charge via the Internet at http://pubs.acs.org.

References and Notes

(1) Kotz, J.; Kosmella, S.; Beitz, T. *Prog. Polym. Sci.* **2001**, *26*, 1199.
(2) Grassl, B.; Billon, L.; Borisov, O.; Francois, J. *Polym. Int.* **2006**, *55*, 1169.
(3) Dischera, B. M.; Hammera, D. A.; Batesb, F. S.; Dischera, D. E. *Curr. Opin. Colloid Interface Sci.* **2000**, *5*, 125.
(4) Yekta, A.; Winnik, M. A. *Curr. Opin. Colloid Interface. Sci.* **1997**, *2*, 424.
(5) Alexandridis, P. *Curr. Opin. Colloid Interface. Sci.* **1996**, *1*, 490.
(6) (a) Nishiyama, N.; Kataoka, K. *Adv. Polym. Sci.* **2006**, *193*, 67. (b) Torchilin, V. P. *Cell Mol. Life Sci.* **2004**, *61*, 2549. (c) Lukyanov, A. N.; Torchilin, V. P. *Adv. Drug Delivery Rev.* **2004**, *56*, 1273. (d) Popot, J.-L.; Berry, E. A.; Charvolin, D.; Creuzenet, C.; Ebel, C.; Engelman, D. M.; Flötenmeyer, M.; Giusti, F.; Gohon, Y.; Hervé, P.; Hong, Q.; Lakey, J. H.; Leonard, K.; Shuman, H. A.; Timmins, P.; Warschawski, D. E.; Zito, F.; Zoonens, M.; Pucci, B.; Tribet, C. *Cell Mol. Life Sci.* **2003**, *60*, 1559.
(7) Velichkova, R. S.; Christova, D. C. *Prog. Polym. Sci.* **1995**, *20*, 819.
(8) Laschewsky, A. *Adv. Polym. Sci.* **1995**, *124*, 1.

(9) (a) Yusa, S.; Sakakibara, A.; Yamamoto, T.; Morishima, Y. *Macromolecules* **2002**, *35*, 10182. (b) Noda, T.; Morishima, Y. *Macromolecules* **1999**, *32*, 4631.
(10) Morishima, Y.; Nomura, S.; Ikeda, T.; Seki, M.; Kamachi, M. *Macromolecules* **1995**, *28*, 2874.
(11) Kujawa, P.; Audibert-Hayet, A.; Seld, J.; Candau, F. *Macromolecules* **2006**, *39*, 384.
(12) McCormick, C. L. *Stimuli.-Responsive. Water Soluble and Amphiphilic Polymers*; American Chemical Society: Washington, DC, 2001.
(13) (a) Yusa, S.; Sakakibara, A.; Yamamoto, T.; Morishima, Y. *Macromolecules* **2002**, *35*, 5243. (b) Yusa, S.; Sakakibara, A.; Yamamoto, T.; Morishima, Y. *Macromolecules* **2002**, *35*, 10182. (c) Yusa, S.; Shimada, Y.; Mitsukami, Y.; Yamamoto, T.; Morishima, Y. *Macromolecules* **2003**, *36*, 4208.
(14) (a) Selb, J.; Biggs, S.; Renoux, D.; Candau, F. *Adv. Chem. Ser.* **1996**, *248*, 251. (b) Candau, F.; Selb, J. *Adv. Colloid Interface Sci.* **1999**, *79*, 149.
(15) Branham, K. D.; McCormick, C. L. *ACS Symp. Ser.* **1995**, *598*, 551.
(16) Gohy, J.-F. *Adv. Polym. Sci.* **2005**, *190*, 65.
(17) Riess, G. *Prog. Polym. Sci.* **2003**, *28*, 1107.
(18) (a) Volpert, E.; Selb, J.; Candau, F. *Macromolecules* **1996**, *29*, 1452. (b) Candau, F.; Regalado, E. J.; Selb, J. *Macromolecules* **1998**, *31*, 5550. (c) Regalado, E. J.; Selb, J.; Candau, F. *Macromolecules* **1999**, *32*, 8580.
(19) Zhang, Y. X.; Wu, F. P.; Li, M. Zh.; Wang, E. J. *J. Phys. Chem. B* **2005**, *109*, 22250.
(20) Hashidzume, A.; Kawaguchi, A.; Tagawa, A.; Hyoda, K.; Sato, T. *Macromolecules* **2006**, *39*, 1135.
(21) (a) Morishima, Y. *Prog. Polym. Sci.* **1990**, *15*, 949. (b) Hashidzume, A.; Yamamoto, H.; Mizusaki, M.; Morishima, Y. *Polym. J.* **1999**, *31*, 1009. (c) Liu, R. C. W.; Winnik, F. M. *J. Photochem. Photobiol. A: Chem.* **2006**, *178*, 208.
(22) (a) Tribet, C.; Audebert, R.; Popot, J.-L. *Proc. Natl. Acad. Sci. U.S.A.* **1996**, *93*, 15047. (b) Tribet, C.; Audebert, R.; Popot, J.-L. *Langmuir* **1997**, *13*, 5570. (c) Gohon, Y.; Giusti, F.; Prata, C.; Charvolin, D.; Timmins, P.; Ebel, C.; Tribet, C.; Popot, J.-L. *Langmuir* **2006**, *22*, 1281.
(23) Matyjaszewski, K.; Xia, J. *Chem. Rev.* **2001**, *101*, 2921.
(24) Nakano, T.; Matsuda, A.; Okamoto, Y. *Polym. J.* **1996**, *28*, 556−558.
(25) (a) Lutz, J.-F.; Jakubowski, W.; Matyjaszewski, K. *Macromol. Rapid Commun.* **2004**, *25*, 486. (b) Isobe, Y.; Yamada, K.; Nakano, T.; Okamoto, Y. *Macromolecules* **1999**, *32*, 5979.
(26) Lutz, L.-F.; Jakubowski, W.; Matyjaszewski, K. *Macromol. Rapid Commun.* **2004**, *25*, 486.
(27) Xie, X.; Hogen-Esch, T. E. *Macromolecules* **1996**, *29*, 1734.
(28) Magny, B.; Lafuma, F.; Iliopoulos, I. *Polymer* **1992**, *33*, 3151.
(29) Pouliquen, G.; Tribet, C. *Macromolecules* **2006**, *39*, 373.
(30) Kumar, S.; Aswal, V. K.; Singh, H. N.; Goyal, P. S.; Kabir-ud-Din *Langmuir* **1994**, *10*, 4069.
(31) (a) Volpe, R. A.; Frisch, H. L. *Macromolecules* **1987**, *20*, 1747. (b) Frisch, H. L.; Xu, Q. *Macromolecules* **1992**, *25*, 5145.
(32) Hill, A.; Candau, F.; Selb, J. *Macromolecules* **1993**, *26*, 4521.
(33) Chang, Y.; McCormick, C. L. *Macromolecules* **1993**, *26*, 6121.
(34) Brinkhuis, R. H. G.; Schouten, A. J. *Langmuir* **1992**, *8*, 2247.
(35) Kevelam, J.; van Breemen, J. F. L.; Blokzijl, W.; Engberts, J. B. F. N. *Langmuir* **1996**, *12*, 4709.
(36) Luccardini, C.; Tribet, C.; Vial, F.; Marchi-Artzner, V.; Dahan, M. *Langmuir* **2006**, *22*, 2304.
(37) (a) Rubinstein, M.; Dobrynin, A. V. *Macromolecules* **2000**, *33*, 8097. (b) Borisov, O. V.; Halperin, A. *Curr. Opin. Colloid Interface Sci.* **1998**, *3*, 415. (c) Borisov, O. V.; Zhulina, E. B. *Macromolecules* **2005**, *38*, 2506.
(38) Petit, F.; Iliopoulos, I.; Audebert, R. *Polymer* **1998**, *39*, 751.
(39) Feng, Y.; Billon, L.; Grass, B.; Bastiat, G.; Borisov, O.; Francois, J. *Polymer* **2005**, *46*, 9283.

MA070397S